Avalanches in the athermal 2d Random-Field Ising model: front propagation versus nucleation and growth dynamics

Author: Víctor Navas Portella
Facultat de Física, Universitat de Barcelona, Diagonal 645, 08028 Barcelona, Spain.

Advisor: Dr. Eduard Vives i Santa-Eulalia

The two-dimensional zero-temperature Random Field Ising Model with local adiabatic relaxation dynamics is studied. When externally driven, this model allows to analyse the properties of an advancing front for different amounts of disorder. By imposing special forced boundary conditions and allowing for systems with rectangular geometry, we favour the existence of a unique interface which is the boundary of a 1d spanning avalanche. We show that the description of an advancing front in terms of a univalued function $x(y)$ lacks of a relevant contribution in the thermodynamic limit: the existence of overhangs and islands which are characteristic of the nucleation and growth dynamics.

I. INTRODUCTION

The athermal (T=0) Random Field Ising Model (RFIM) has been commonly used to explain the Barkhausen noise in ferromagnetic materials [1][2]. In many cases, ferromagnetic coupling is so strong that it is not necessary to consider temperature as a relevant parameter in the model. Energy barriers are large enough that thermally activated processes are negligible. By considering interaction between spins, quenched disorder in the sample and external magnetic field, this model offers a good explanation of hysteresis and crackling noise (avalanche dynamics).
This model is applicable to other physical systems such as structural transitions, superconductivity, capillary condensation of gases in porous solids, etc. [2][3]. In all these experiments there is a first order phase transition and hysteresis process occurs. Metastable states separated by high energy barriers appear in the free energy landscape. The effect of quenched disorder determines which sites of the system are more favourable to nucleate or not under the presence of a perturbation. When an external force is applied, for example a magnetic field, a discontinuity in the conjugated variable, for example magnetization, appears as a system response. This non-equilibrium collective event, known as an 'avalanche', is essentially due to the fact that the system jumps from one metastable state to another. The properties of these avalanches depend strongly on the quenched disorder present in the system.
The RFIM with Periodic Boundary Conditions (PBC) describes a first order phase transition dynamics through a pure nucleation process. The lower critical dimension of the RFIM is known to be $d_c = 2$ in the equilibrium case [4]. This implies that ferromagnetic order will not be present for $d \leq 2$ in this model. What is not totally clear is if the lower critical dimension is still $d_c = 2$ for the RFIM with local metastable dynamics at T=0. Sethna opened the door to a possible existence of long range order in this model [5]. Nevertheless, it was necessary to examine larger system sizes in order to determine whether the critical value associated to the quenched disorder σ_c in the thermodynamic limit was finite or not. Recently, Spasojević et al. found numerical evidence of a critical point below which the system orders ferromagnetically. These evidences were based on the finite size scaling collapse of the curves corresponding to magnetization [6], distribution of avalanche sizes [7] and number of spanning avalanches [8].
On the other hand, Seppälä et al. [9] found evidence of roughening effects in the equilibrium RFIM at $T = 0$ with Forced Boundary Conditions (FBC) without external field. The model with metastable dynamics but restricted to nucleation close to the interface, was studied in the context of depinning transition [10], and for the study of morphological changes in the invading front [11].
In this work, we present a different point of view to deepen the understanding of these phenomena. By applying FBC to the athermal RFIM with metastable dynamics and changing the geometry of the system from square to rectangular, the presence of the critical transition (order-disorder) and the roughening transition are studied. The model with FBC is intermediate between a pure nucleation process and a single interface dynamics. Nucleation of domains away from the propagating front is allowed as well as the presence of overhangs. As it will be shown, the use of rectangular systems allows to separate roughening and order-disorder transitions and combined finite size scaling hypothesis will be contrasted.
This manuscript is structured as follows: Section II presents the model and simulation details. Results with partial curve collapse are presented in Section III. Conclusions and a brief summary of the results are exposed in Section IV.

II. MODEL

From a general point of view, Ising models consist in an ensemble of N interactive spins situated at the nodes of a d-dimensional lattice. The RFIM is a variant of these kind of models which includes quenched disorder that

distorts the free energy landscape. For this purpose, one considers a random field h_i associated to each node of the lattice which represents a defect: impurities, dislocations, frustration, vacancies, etc. Spins can take the values $s_i = \pm 1$. The Hamiltonian describing this model is:

$$\mathcal{H} = -\sum_{\langle ij \rangle} J s_i s_j - \sum_i (H + h_i) s_i. \quad (1)$$

The first term accounts for ferromagnetic interaction with nearest neighbours. For simplicity, we consider $J = 1$. H is the external field and $\{h_i\}$ are local quenched random fields, Gaussian distributed according to:

$$\rho(h) = \frac{1}{\sqrt{2\pi\sigma^2}} exp\left(-\frac{h^2}{2\sigma^2}\right), \quad (2)$$

where σ characterizes the amount of disorder present in the system. In this work a 2d square lattice with rectangular shape ($N = L_x \times L_y$) is studied. The aspect ratio a is defined as $a = \frac{L_y}{L_x}$. In order to generate a metastable dynamics, it is necessary to stablish a criterion to determine under which conditions the system remains in a local minimum of the free energy landscape. A spin is stable when it is aligned with its effective field:

$$h_i^{eff} = \sum_k^z s_k + H + h_i, \quad (3)$$

where z is the coordination number, which in the case of a 2-d square lattice is $z = 4$. Following this deterministic rule, a spin flips when its local field changes sign. A flipping event changes the effective field of the nearest neighbours and any of these could become unstable. The process continues in the same way originating an avalanche of flipping spins. The number of spins that have changed their state in the same avalanche defines the size of the avalanche. Simulations start with all the spins pointing down ($\{s_i\} = -1$) and $H = -\infty$. The external field is increased until a spin triggers an avalanche. Then the external field is kept constant until there are no more unstable spins and the system reaches a metastable state again. The dynamical process finishes when all the spins are pointing up ($\{s_i\} = +1$) and $H = +\infty$. For numerical simulations, the Sorted list algorithm has been used [12]. Instead of simulating extremely large systems, it has been preferable to study characteristic sizes of $L_x, L_y \leq 1024$ and perform a large number of averages over randomness realizations.

For the study of avalanches it is important to distinguish those which span the system in one or two spatial dimensions from the non-percolating ones. In the thermodynamic limit, spanning avalanches are candidates to represent critical effects or discontinuities in the magnetization. A 1d spanning avalanche is defined as that event which follows a connecting-path between opposite sides of the system. Since the lattice has rectangular shape, 1d spanning avalanches in the $\hat{x}$ direction (N_1^x) and 1d spanning avalanches in the $\hat{y}$ direction (N_1^y) must be distinguished. If the event connects all four sides then it is considered as a 2d spanning avalanche. With the standard PBC and $L_x = L_y \equiv L$, this model has been broadly studied [5]-[8]. Recent numerical results indicate that there exists a continuous transition for a finite value of disorder $\sigma_c = 0.54$ which separates two different regimes [5][6]. For $\sigma < \sigma_c$, there is an infinite avalanche, which is usually 2-d spanning (See Fig. 1 (a)). When disorder reaches its critical value σ_c, there is a peak in the average number of 1d spanning avalanches [8]. Power-law distributions are found in some magnitudes related to avalanches in this situation (size and duration). For the regime $\sigma > \sigma_c$, the magnetization process takes place by nucleation of small domains and there is no presence of spanning avalanches (See Fig. 1 (b)).

The idea of imposing non-standard FBC is to force simulations to exhibit a domain wall which can be identified as an advancing front (See Fig. 1 (c) and (d)). From a physical point of view, FBC would represent a situation in which the system under study is a subset of a bigger one with an already formed interface. FBC consists in keeping PBC in the vertical $\hat{y}$ direction whereas the horizontal $\hat{x}$ direction is subjected to fixed boundaries: at the extreme $x = L_x + 1$, there is a row of up spins whereas at $x = 0$ one assumes that there is a row of down spins. Under these specific conditions, 1d spanning avalanches in the $\hat{y}$ direction are more common in a regime of low disorder. Below a certain value of the quenched disorder, σ_r, a sequence of flat 1d massive spanning avalanches appears magnetizing the system (See Fig. 1 (c)). As disorder increases, non-spanning avalanches also take place and 1d spanning avalanches become progressively not as massive and less common. In this second regime, a rough interface can still be identified (See Fig. 1 (d)). As disorder is close to σ_c, critical 1d spanning avalanches appear as a reminiscence of the model with PBC. In a high disorder regime, the presence of 1d spanning avalanches has practically no statistical weight and it is not possible to identify a propagating front any more. In this last regime, nucleation and growth dynamics is recovered, as in the case with PBC (See Fig. 1 (e)).

Interface properties can be studied when 1d spanning avalanches in the $\hat{y}$ direction occur. In such situation, two front lines can be defined by a single-valued function $x(y)$. The right (I_R) and left (I_L) interfaces are defined as follows:

- I_R : Right interface of the 1d spanning avalanche. For every value of y the position of the front is set at the most right spin of the spanning avalanche.

- I_L : Left interface of the 1d spanning avalanche. For every value of y the front is located at the most left position of the spanning avalanche.

See the example in Fig. 2 where the spanning avalanche (green coloured) and the fronts I_L and I_R are plotted. Roughness of I_L and I_R are independently measured by

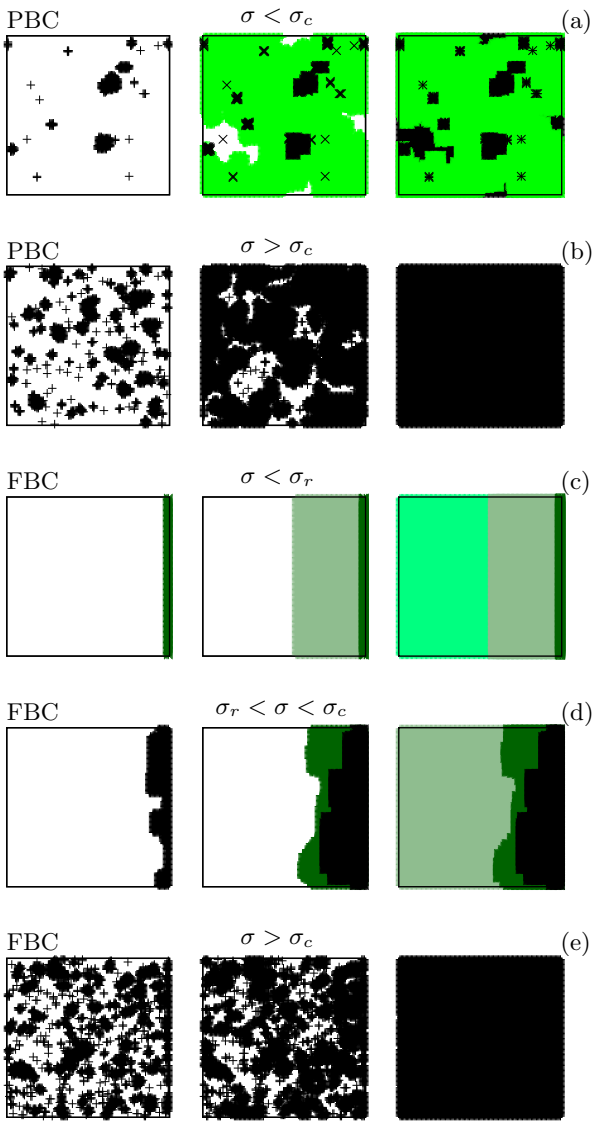

FIG. 1. Sequence of configurations during the magnetization process for PBC (pure nucleation) and FBC (front propagation). External field H is increased from left to right bringing the system from negative magnetization (white regions) to positive magnetization (coloured regions). Black coloured spins correspond to non spanning avalanches. Green regions are spanning avalanches. In (c) and (d) the interface advances from right to left. Different tones of green represent different 1d spanning avalanches.

using the following relation:

$$\omega = \sqrt{\frac{1}{L_y}\sum_{j=1}^{L_y} x^2(j) - \left(\frac{1}{L_y}\sum_{j=1}^{L_y} x(j)\right)^2}, \qquad (4)$$

where $x(j)$ represents the x coordinate corresponding to the position of the interface at a fixed height $y = j$.
The description of the interface in terms of two univalued lines $x(y)$ does not account for the existence of overhangs, unflipped regions, and flipped regions that were present prior to the avalanche. For each spanning avalanche, one can measure the number of spins which have flipped $n\uparrow$, the area A enclosed between I_R and I_L and the magnetization inside this area M_A. The connected topology of 1d spanning avalanches can leave unflipped regions (U) behind the final interface I_L (white islands in Fig. 2) and it can enclose islands that were already flipped (F) before the avalanche event (darker regions in Fig. 2). The present study allows to compute these defects. Taking into account that $M_A = n\uparrow + F - U$, the quantities Δ, U and F can be evaluated by using the following relations:

$$\Delta = A - n\uparrow = U + F, \qquad (5)$$

$$U = \frac{1}{2}\left(\Delta + n\uparrow - M_A\right), \qquad (6)$$

$$F = \frac{1}{2}\left(\Delta - n\uparrow + M_A\right). \qquad (7)$$

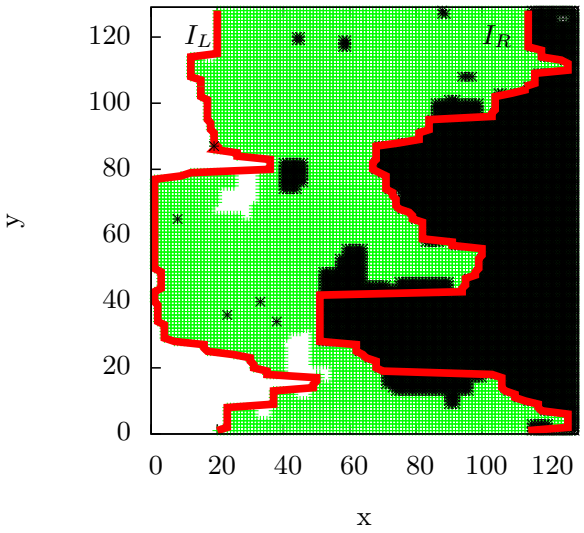

FIG. 2. Configuration of a system (L=128,$\sigma = 0.85$) in which a 1d spanning avalanche advancing from right to left has occurred. Same color code as in Fig. 1. Interfaces are highlighted with red lines.

In the following sections, in order to obtain reliable statistics, averages are taken over a number of randomness realizations which is of the order of 10^5.

III. RESULTS

A. 1d Spanning avalanches

The average number of 1d spanning avalanches as a function of the disorder σ is presented in Fig. 3 (a) for PBC in square systems ($L_x = L_y; a = 1$).

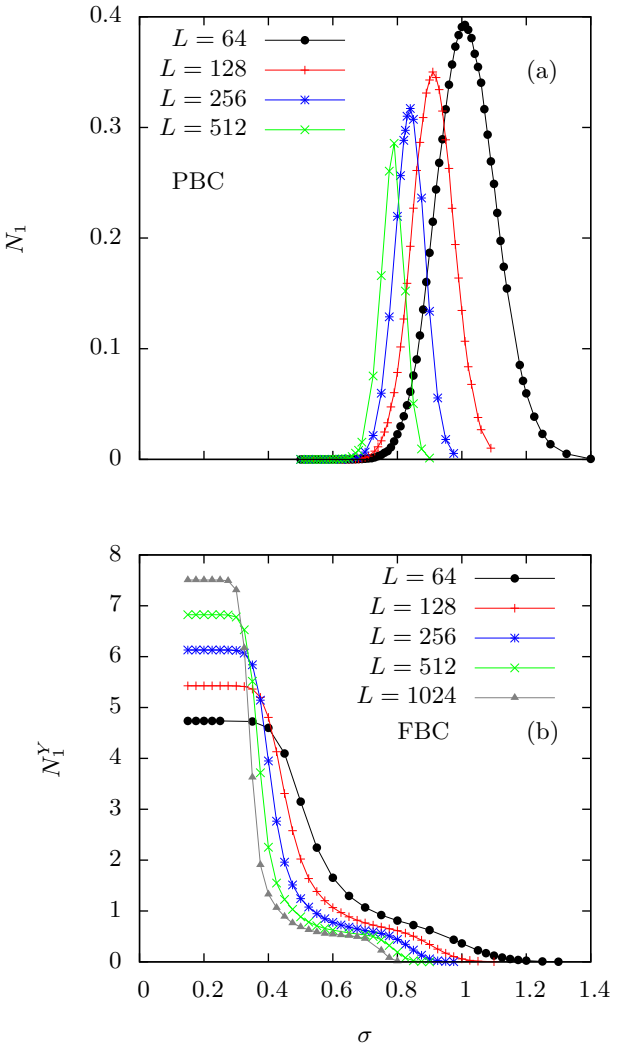

FIG. 3. Average number of 1d spanning avalanches per run against the disorder σ for different system sizes in a square system $a = 1$ for PBC (a) and for FBC (b). Lines are guides to the eye.

The number of 1d spanning avalanches exhibits a peak at the value of disorder $\sigma_c(L)$ as it was found by Spasojević et al. in Ref. [8]. These peaks present the following scaling behaviour:

$$N_1^{PBC}(\sigma, L) = L^{\theta_c} G^{PBC}\left(L^{1/\nu_c}\frac{\sigma - \sigma_c}{\sigma}\right), \qquad (8)$$

where $\sigma_c = 0.54 \pm 0.03$, $\frac{1}{\nu_c} = 0.19 \pm 0.02$, $\theta_c = -0.10 \pm 0.03$ and $G^{PBC}(z)$ is a scaling function related to the number of 1d spanning avalanches for PBC (See Fig. 5 (b)). Note that the negative value of θ_c means tat 1d spanning avalanches are negligible in the thermodynamic limit.
The number of 1d spanning avalanches in the $\hat{y}$ direction is shown in Fig. 3 (b). A minuscule fraction of 1d spanning avalanches in the $\hat{x}$ direction as well as 2d spanning avalanches are also found but with no relevant statistical weight. A handwaving argument to explain why there are more 1d spanning avalanches in the model with FBC than with PBC is given as follows: in the low disorder regime, local fields take values around zero. As spins near the boundary $x = L_x$ have a neighbour which is pointing up the external field needs to be around $H = 2$ in order to flip it and create a nucleation site for a 1d spanning avalanche to propagate from $y = 0$ to $y = L_y$. Contrarily, in the model with PBC, the external field needs to be around $H = 4$ in order to flip a spin generating the same spanning avalanche. As it can be appreciated in Fig. 3 (b), two steps are present in the number of 1d spanning avalanches with FBC. The higher (left) step is related to a morphological transition of the propagating front. This transition separates the regimes where there is a sequence of 1d spanning avalanches with a flat profile (faceted growth) and the regime where 1d spanning avalanches exhibit a certain rough profile. The second step occurs in the same region where data for PBC shows a peak (Fig. 3 (a)) and it can be understood as a signature of the bulk critical transition. In order to elucidate how the height of the step related to roughening effects depends on the system size and shape, simulations at different L_x and L_y have been performed. In Fig. 4, one can appreciate that L_x controls the height of this step. By changing the aspect ratio, the morphology of the curves is varied. When a is lower than unity, which means that the surface is dominated by periodic boundaries, critical effects are strengthened. As the aspect ratio increases, the sides of the system which are subjected to forced boundary conditions take over and critical effects are gradually hindered.

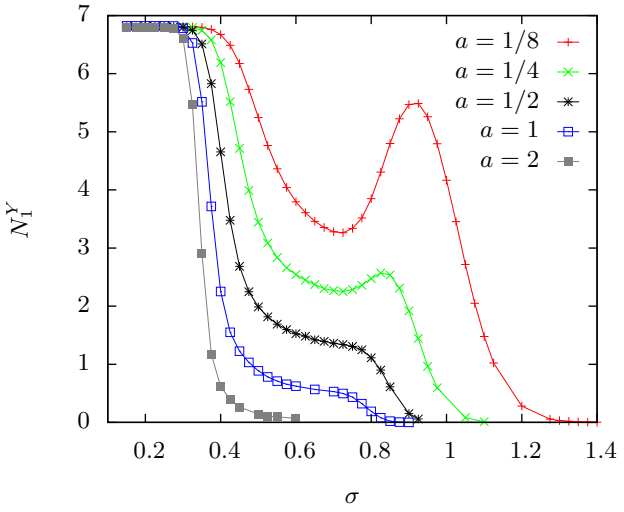

FIG. 4. Average number of 1d spanning avalanches per run in a system with a fixed $L_x = 512$ and different aspect ratio $a = L_y/L_x$. Lines are guides to the eye.

The presence of these transitions suggests proposing combined finite size scaling relations with parameters related to both transitions in order to achieve partial

curve collapse. For a fixed geometry of the system, i.e. same aspect ratio, the scaling relation for 1d spanning avalanches with FBC through which partial curve collapse is achieved reads:

$$N_1^Y(\sigma, L_x, L_y) = L_x^{\theta_r}\tilde{G}\left(L_x^{1/\nu_r}\frac{\sigma-\sigma_r}{\sigma_r}; a\right) + (L_xL_y)^{\theta_c/2}\,\tilde{\tilde{G}}\left((L_xL_y)^{1/2\nu_c}\,\frac{\sigma-\sigma_c}{\sigma}; a\right). \quad (9)$$

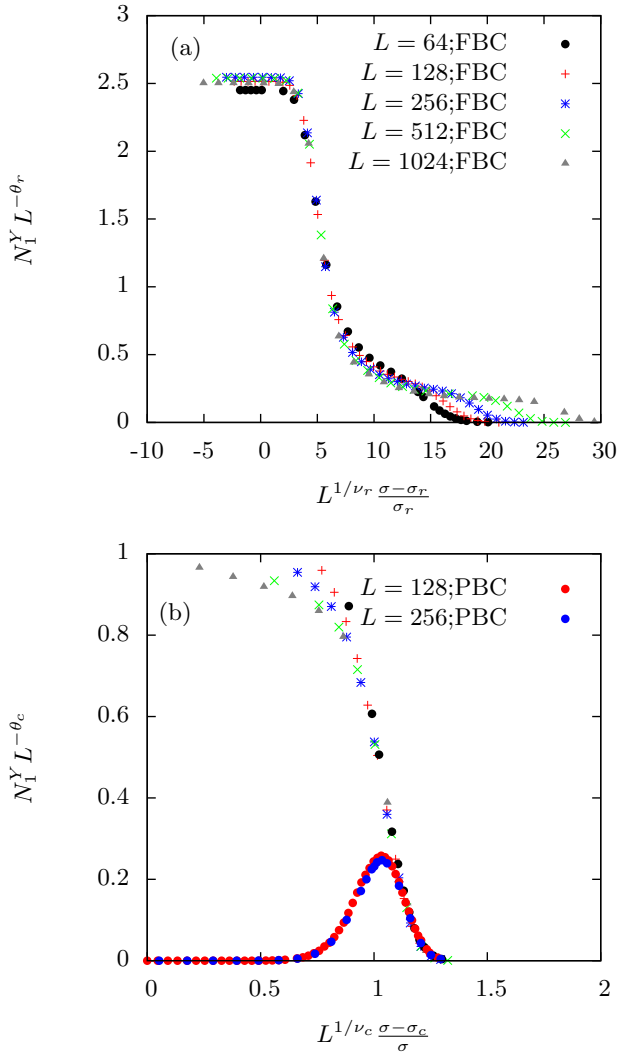

FIG. 5. Partial curve collapse of the average number of 1d spanning avalanches per run for different system sizes in a square lattice $L_x = L_y \equiv L$. Partial curve collapse in the regime dominated by roughening effects is presented in (a). Partial curve collapse for the regime dominated by the bulk critical transition is shown in (b). Scaled PBC peaks are presented reduced by a factor 1/2, as Eq. (10) indicates (Note that $G^{PBC}(z;1) = 2\tilde{\tilde{G}}^{FBC}(z;1)$ for $a = 1$).

Partial curve collapse is achieved in the roughening regime under the set of parameters $\sigma_r = 0.25 \pm 0.02$, $\frac{1}{\nu_r} = 0.37 \pm 0.02$ and $\theta_r = 0.16 \pm 0.01$ (See Fig. 5 (a)). The scaling function in this regime, $\tilde{G}(z;a)$ depends on the aspect ratio and the scaling variable $z = L_x^{1/\nu_r}\frac{\sigma-\sigma_r}{\sigma_r}$ which depends on the length L_x. All errors associated to the set of scaling parameters represent the approximate range for which collapses are still satisfactory (This definition is valid for the following scaling collapses presented in this work). In the thermodynamic limit, the number of flat spanning avalanches diverges near σ_r. This divergence is not surprising since, as L_x becomes larger, the number of 1d spanning avalanches in the $\hat{y}$ direction that can fit in the system increases. Partial curve collapse is achieved in the bulk critical regime under the set of parameters from Eq. (8). (See Fig. 5 (b)). The scaling function in this regime, $\tilde{\tilde{G}}(z;a)$ is strongly-dependent on the aspect ratio a. The scaling variable in this case, $z = (L_xL_y)^{1/2\nu_c}\,\frac{\sigma-\sigma_c}{\sigma}$, has been defined from the geometrical average length $\sqrt{L_xL_y}$, so as to evidence the spatial isotropy related to this critical transition. The hypothesis of combined finite size scaling remains still valid for different aspect ratios where the critical effects have more presence (Fig. 6) or have practically disappeared (Fig. 7). The connection between 1d critical spanning avalanches in the model with FBC with those in the model with PBC, is justified by a numerical evidence: the right tail of the peak found with PBC is related with that one found with FBC by the following equation:

$$G^{PBC}(z;a) = \tilde{\tilde{G}}^{FBC}(z;a) + \tilde{\tilde{G}}^{FBC}\left(z;\frac{1}{a}\right), \quad (10)$$

where z, is the scaling variable in the critical regime and $G^{PBC}(z,a)$ and $\tilde{\tilde{G}}^{FBC}(z;a)$ are scaling functions in the critical regime for PBC and FBC (See Fig. 5 (b) and Fig. 6 (b)). This relation is justified by the geometrical independence of the bulk critical transition in PBC, $\tilde{\tilde{G}}^{PBC}(z;a) = \tilde{\tilde{G}}^{PBC}\left(z;\frac{1}{a}\right)$, and by the symmetry breaking due to the presence of FBC, $\tilde{\tilde{G}}^{FBC(X;Y)}_{Y;X}(z;a) = \tilde{\tilde{G}}^{FBC(Y;X)}_{X;Y}\left(z;\frac{1}{a}\right)$, where the superscripts $FBC(X,Y)$ represent a system with fixed boundaries in the $\hat{x}$ or $\hat{y}$ directions and the subscripts X and Y correspond to the scaling functions related to 1d spanning avalanches in those directions.

From the behaviour for 1d spanning avalanches in systems with stripe geometry ($a < 1$), four different regimes can be distinguished as a function of the disorder σ. First, there is the faceted growth regime at $\sigma < \sigma_r$ (Fig. 8 (a)). A second regime at $\sigma_r < \sigma < \sigma_c$ where the advancing front presents a rough profile and there is a meaningless presence of nucleated domains in front of the advancing interface (Fig. 8 (b)). A third regime at $\sigma \sim \sigma_c$ where the critical interface advances under the existence of nucleated domains (Fig. 8 (c)). Above σ_c, it is unlikely to find a 1d spanning avalanche in order to define a front and thus, the front will be ill-defined (Fig. 8 (d)). For higher disorders, nucleation and growth dynamics is recovered.

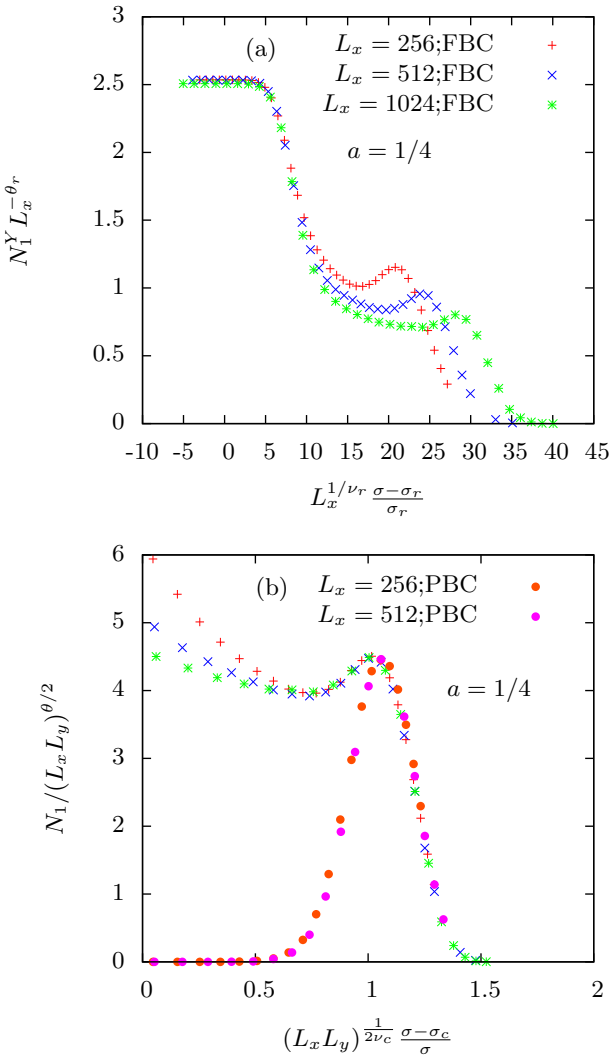

FIG. 6. Partial curve collapse of the average number of 1d spanning avalanches per run for different system sizes with $a = 1/4$. Partial curve collapse in the regime dominated by roughening is presented in (a). Partial curve collapse for the regime dominated by the bulk critical transition is shown in (b). Peaks of PBC are superposed in the critical regime following Eq. (10) for $a = 1/4$. Note that $\tilde{\tilde{G}}^{FBC}(z, \frac{1}{a} = 4) \to 0$.

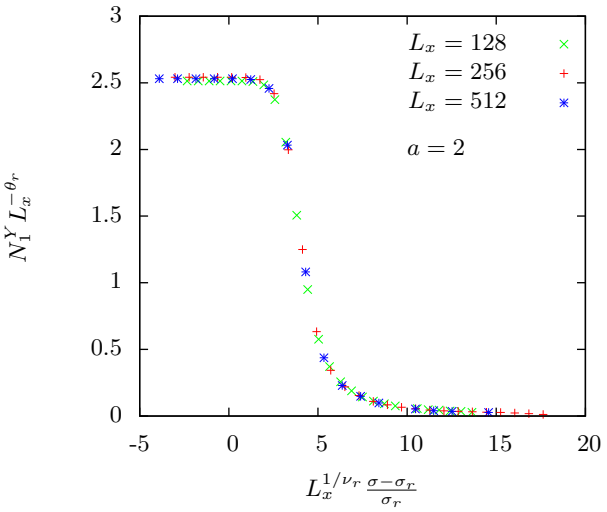

FIG. 7. Curve collapse for average number of 1d spanning avalanches per run for different system sizes in a system with $a = 2$. In this case, critical effects have been hindered and the contribution of spanning avalanches in the critical region is meaningless.

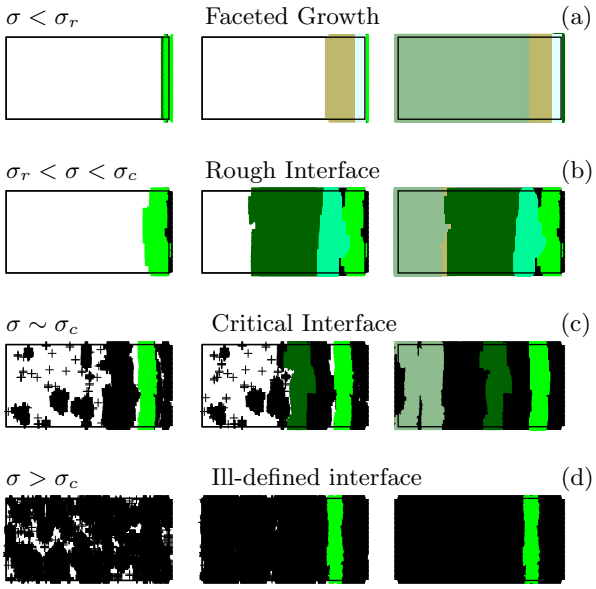

FIG. 8. Sequence of configurations during the magnetization process for FBC model with aspect ratio $a = 1/8$. External field H is increased from left to right. Black coloured regions correspond to non-spanning avalanches whereas 1-d spanning avalanches are represented by different tones of green.

B. Interface analysis

1. *Roughness curves*

Results of the roughness curves for square systems $a = 1$ ($L_x = L_y \equiv L$) are presented in this subsection. In Fig. 9, one can appreciate the roughness curves for a system of size $L = 512$. This quantity can be understood as an order parameter which describes the transition from faceted growth to rough interface. Below σ_r, ω is null and a faceted growth is identified whereas a rough interface appears above σ_r. In the region dominated by bulk critical effects (right hand side of Fig. 9), these roughness curves exhibit a peak.

At a given disorder σ, the average value of the effective width of the interface I_R is higher than I_L, $\omega_R > \omega_L$. This fact can be explained by understanding how fronts have been pinned. The interface I_L is essentially pinned by very negative random fields and small nucleated do-

mains whereas I_R is stopped by large regions that were already flipped in small independent avalanches. Such a random spatial boundary confers a higher effective width to this front line.

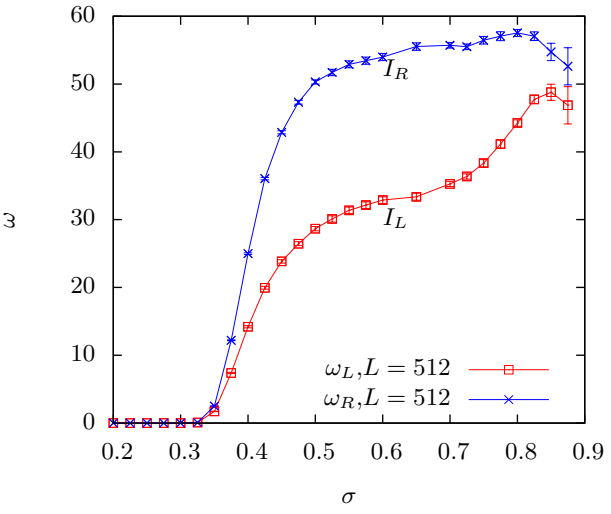

FIG. 9. Average roughness of both interfaces as a function of the disorder σ for a square system of L=512. Lines are guides to the eye.

The identification of features related to both transitions in these curves suggests again using partial curve collapse by proposing the following combined scaling relations.

$$\omega_R(\sigma, L) = L^{\zeta_r^R} \tilde{W}_r^R \left(L^{1/\nu_r} \frac{\sigma - \sigma_r}{\sigma_r} \right) + L^{\zeta_c^R} \tilde{W}_c^R \left(L^{1/\nu_c} \frac{\sigma - \sigma_c}{\sigma} \right), \quad (11)$$

$$\omega_L(\sigma, L) = L^{\zeta_r^L} \tilde{W}_r^L \left(L^{1/\nu_r} \frac{\sigma - \sigma_r}{\sigma_r} \right) + L^{\zeta_c^L} \tilde{W}_c^L \left(L^{1/\nu_c} \frac{\sigma - \sigma_c}{\sigma} \right), \quad (12)$$

where W_r^R,W_r^L, W_c^R and W_c^L are the scaling functions for both interfaces I_R and I_L in the roughening (r) and bulk critical regime (c). Partial curve collapses are presented in Fig. 10 and Fig. 11 and the fitted roughness exponents are presented in Tab. I. In the faceted growth regime, 1d critical spanning avalanches present a null roughness exponent ($\zeta^R = 0$, $\zeta^L = 0$). Due to finite size effects, null values of the effective width are found. As exposed by Ji and Robbins in Ref. [11], the propagating front exhibits a non-null value of roughness at sufficiently large length scales for Gaussian quenched disorder although our system sizes do not allow to observe it. Roughness exponents in the regime where the rough interface advances under the presence of few nucleated domains ($\sigma_r < \sigma < \sigma_c$), $\zeta_r^R = 1.00 \pm 0.02$ and $\zeta_r^L = 1.00 \pm 0.01$,

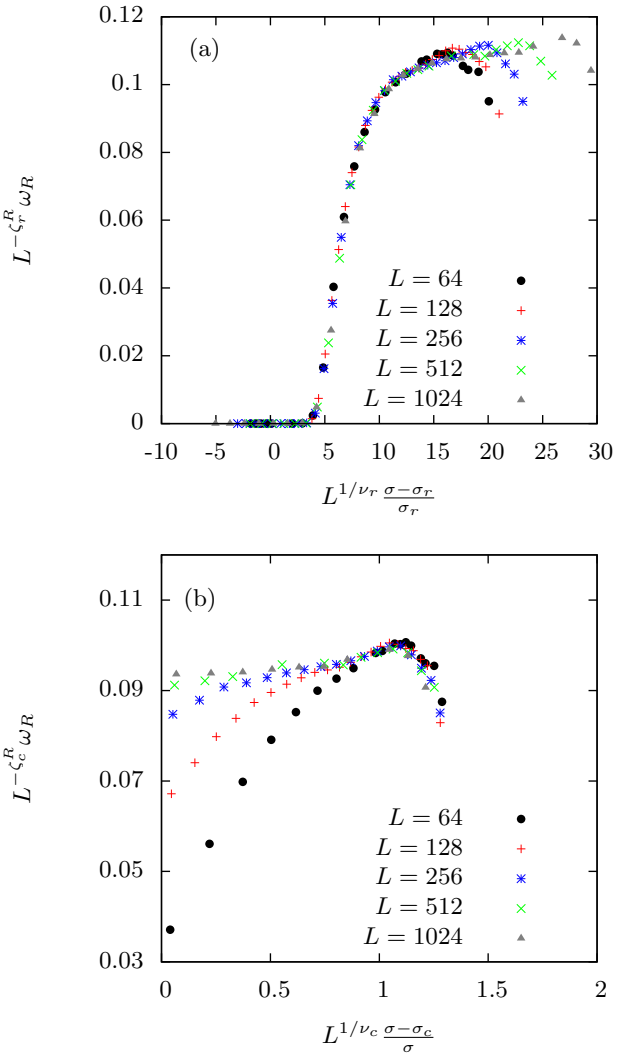

FIG. 10. Partial curve collapse of average roughness of the interface I_R in the regime dominated by roughening effects in (a) and at the region of disorder dominated by critical effects in (b).

match with the exact result predicted by renormalization group theories $\zeta = (5-d)/3\ (=1)$ [13]. For $\sigma \sim \sigma_c$, as it was found in the equilibrium case [9], there are deviations from $\zeta = 1$. In this critical regime, the fitted roughness exponents are $\zeta_c^R = 1.02 \pm 0.01$ and $\zeta_c^L = 0.95 \pm 0.01$. Thus, changes in the morphological properties of critical interfaces are expected.

2. *Overhangs and Islands*

Standard studies of driven interfaces in disordered media using a continuous description $x(y)$ of the interface do not allow for the existence of overhangs [14] nor nucleation away from the front when it is energetically favourable. In some cases, overhangs are permitted but

	$\sigma < \sigma_r$ (Faceted Growth)	$\sigma_r < \sigma < \sigma_c$ (Rough interface)	$\sigma \sim \sigma_c$ (Critical Interface)	$\sigma > \sigma_c$ (Ill-defined Interface)
ζ^R	0	1.00 ± 0.02	1.02 ± 0.01	-
ζ^L	0	1.00 ± 0.01	0.95 ± 0.01	-

TABLE I. Roughness exponents related to interfaces I_R and I_L for all different types of growth.

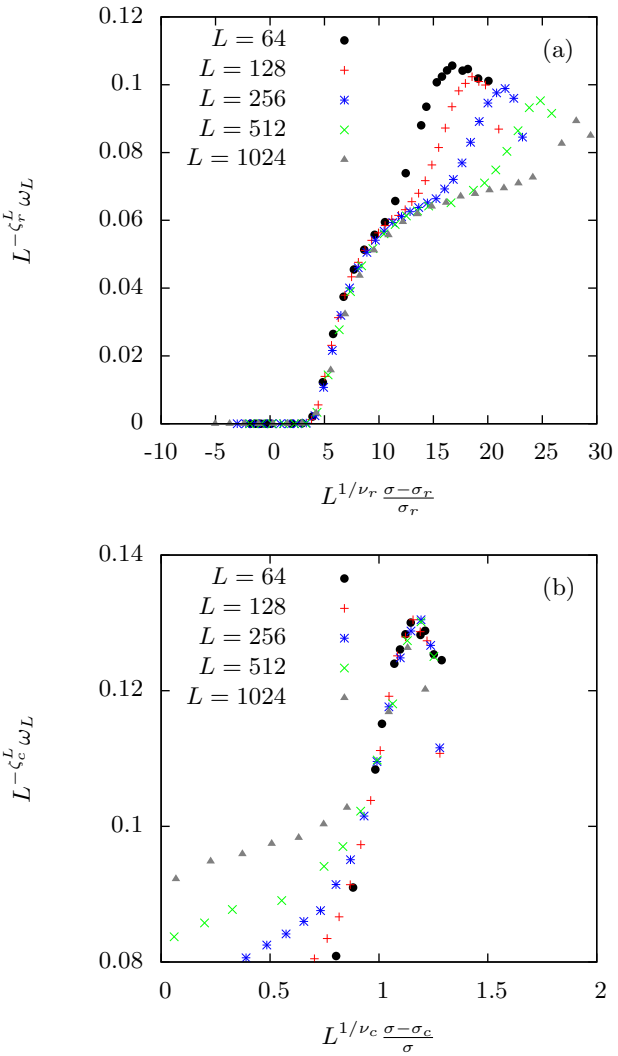

FIG. 11. Partial curve collapse of average roughness of the interface I_L in the regime dominated by roughening effects in (a) and in the region of disorder dominated by critical effects in (b).

not nucleation disconnected from the propagating interface [10][11][15]. Therefore, it is interesting to evaluate the importance of these contributions.

The analysis of unflipped regions left behind (U) the interface comprehends overhangs of the front I_L and unflipped islands with very negative local fields. In Fig. 12 (a), a single peak which grows and shifts to lower values of σ as the system size L is increased can be observed. Despite the fact that one observes a single peak, the finite size scaling collapse is not possible by assuming a unique contribution. Thus, as it has been done in the preceding sections, a combined finite size scaling relation is proposed in order to test partial curve collapse. This scaling relation reads:

$$\frac{U(\sigma,L)}{L^2} = L^{\theta_U^r}\tilde{U}_r\left(L^{1/\nu_r}\frac{\sigma-\sigma_r}{\sigma_r}\right) + L^{\theta_U^c}\tilde{U}_c\left(L^{1/\nu_c}\frac{\sigma-\sigma_c}{\sigma}\right), \tag{13}$$

where $\theta_U^r = -0.2 \pm 0.1$, $\theta_U^c = 0.43 \pm 0.02$ and $\tilde{U}_r$,$\tilde{U}_c$ are scaling functions in the roughening and bulk critical regime. First term in Eq. (13) exhibits good collapse for the left tail of the peak (not shown) whereas the second term shows good collapse in the critical region (See Fig. 12 (b)). Since in this combined finite size scaling relation there is a negative exponent θ_U^r, one concludes that the contribution of U in the roughening regime does not play a significant role in the thermodynamic limit. On the other hand, due to the positive value of the exponent θ_U^c, the fraction of area occupied by overhangs and islands diverges near the critical point.

The analysis of flipped regions in front (F) of the interface includes the contribution of overhangs of the front I_R and isolated flipped islands which had already transformed prior to the spanning avalanche and have been absorbed afterwards. In Fig. 13 (a), two peaks are gradually discriminated as the system size is increased. In the regime $\sigma < \sigma_r$, there are no nucleated islands in front of the interface and no overhangs, which agrees with the existence of the faceted growth regime. In the absence of isolated nucleated domains, the peak situated in the roughening regime corresponds solely to overhangs of the interface I_R. As disorder is approached to σ_c there is a strong presence of nucleated islands in front of the interface. This contribution is manifested in a second peak in this regime of disorder. The existence of two contributions clearly suggests proposing a combined finite size scaling so as to obtain partial curve collapse. The scaling relation reads:

$$\frac{F(\sigma,L)}{L^2} = L^{\theta_F^r}\tilde{F}_r\left(L^{1/\nu_u^r}\frac{\sigma-\sigma_r}{\sigma_r}\right) + L^{\theta_F^c}\tilde{F}_c\left(L^{1/\nu_u^c}\frac{\sigma-\sigma_c}{\sigma}\right), \tag{14}$$

where $\theta_F^r = 0.05 \pm 0.01$, $\theta_F^c = -0.3 \pm 0.2$ and $\tilde{F}_r$, $\tilde{F}_c$ are scaling functions in the roughening and bulk critical regime. The fraction of area occupied by overhangs and islands diverges in the thermodynamic limit in the vicinity of σ_r (See Fig. 13 (b)) whereas the fraction of area occupied by isolated nuclei near σ_c is an irrelevant surface effect.

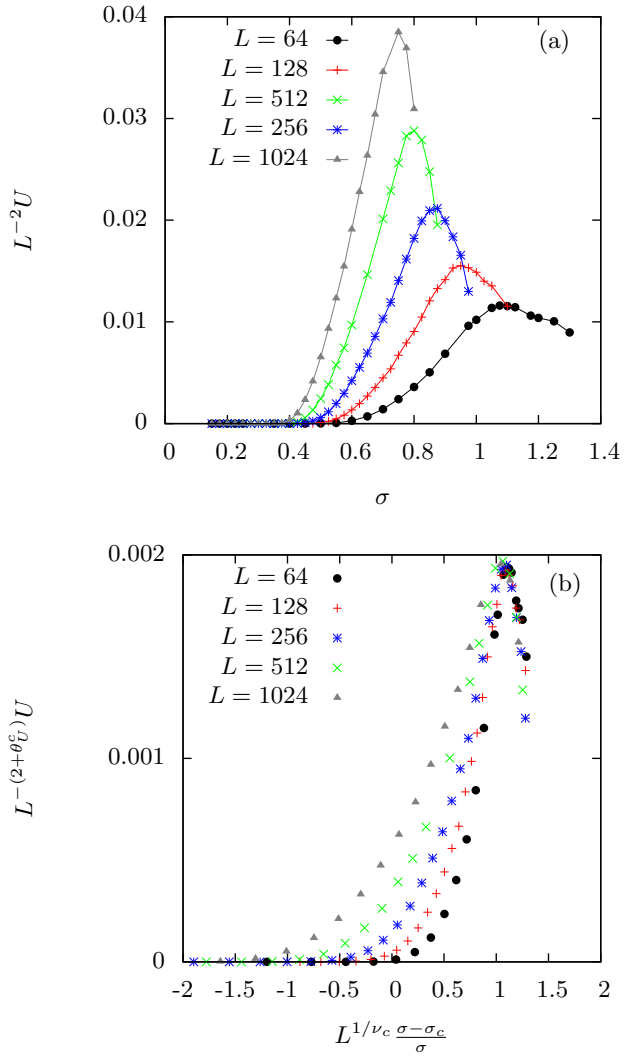

FIG. 12. Average area U of unflipped regions left behind the interface over the total surface of the system against the disorder σ in (a) and partial curve collapse in the region of disorder dominated by critical effects in (b). Lines are guides to the eye.

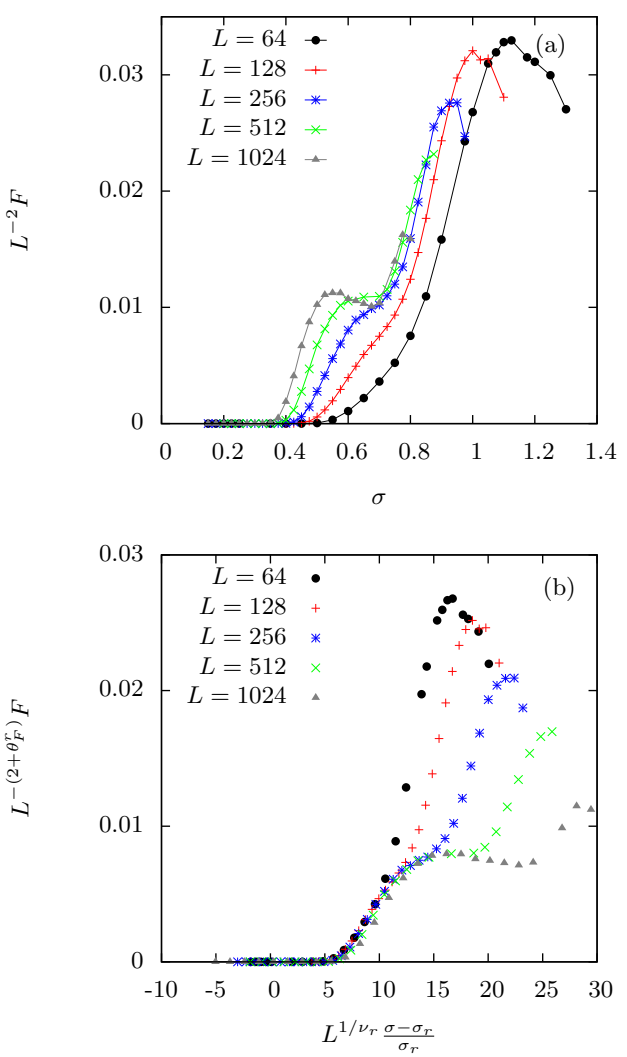

FIG. 13. Average area F of flipped regions left behind the interface over the total surface of the system against the disorder σ in (a) and partial curve collapse in the region of disorder dominated by critical effects in (b). Lines are guides to the eye.

IV. CONCLUSIONS

In this work we have presented results corresponding to the athermal RFIM with local adiabatic relaxation dynamics with FBC and rectangular geometries with different aspect ratios. A transition from faceted growth to rough growth is found at $\sigma_r \cong 0.25$ as well as the order-disorder transition at $\sigma_c \cong 0.54$. The critical effects at σ_c are more important as the aspect ratio L_y/L_x becomes smaller (stripe geometries). Due to the existence of these transitions, combined scaling relations have been proposed and partial curve collapse has been achieved.
In summary, four different propagating front regimes can be observed as a function of increasing disorder. i) The faceted growth regime ($\sigma < \sigma_r$), which presents a null roughness exponent; ii) A rough advancing interface at $\sigma_r < \sigma < \sigma_c$ which presents $\omega_L, \omega_R \sim L$; iii) A critical advancing interface in the bulk critical regime ($\sigma \sim \sigma_c$) which exhibits deviations in the roughness exponents ($\omega_R \sim L^{1.02}$ and $\omega_L \sim L^{0.95}$) and finally iv) a ill-defined interface for higher values of the disorder σ.
Contribution of overhangs and islands has been computed in square systems ($a = 1$). It has been shown that, in the thermodynamic limit, the area occupied by overhangs of the interfaces I_R and flipped islands diverges as $F \sim L^{2.05}$ in the roughening regime ($\sigma_r < \sigma < \sigma_c$). Near σ_c, the area occupied by overhangs of I_L and unflipped islands diverges as $U \sim L^{2.43}$. These divergences suggest that, in order to study critical phenomena in invading front problems using the athermal RFIM with metastable

dynamics, overhangs and islands must be considered.
Further research based on roughness curves and contribution of overhangs and islands for non-squared systems ($a \neq 1$) will give us a better understanding of the competition between front propagation and pure nucleation processes.

ACKNOWLEDGMENTS

This work was completed with computational resources provided by IBERGRID collaboration.
First and foremost, I would like to thank my advisor, Eduard Vives, for his constant support and for encouraging me all the time.
Special thanks go to Djordje Spasojević and Jordi Baró. Their advises and different points of view have enriched this work. I also acknowledge fruitful discussions and good moments with Enric Sanmartí, Pere Arnan and Xavier Roderic Hoffmann.
Very special thanks to my mother Núria Portella, my sister Sònia Navas and my girlfriend Núria Arredondo. Without their love and constant support this work would not have been possible. At last, very special thanks to Nemesio Navas, my father, for teaching me that every new day is a new challenge.

[1] James P. Sethna, Karin Dahmen, Sivan Kartha, James A. Krumhansl, Bruce W. Roberts and Joel D.Shore; *'Hysteresis and Hierarchies: Dynamics of Disorder-Driven First-Order Phase transitions'*. Phys. Rev. Lett. **70**, 3347 (1993)

[2] James P. Sethna, K.A. Dahmen,O.Perkovic in *'The science of Hysteresis* edited by G.Bertotti and I. Mayergoyz, Vol.2, 105-179 (Academic Press, Amsterdam, 2006)

[3] M. Rosinberg and E.Vives, *'Recent topics on metastability, hysteresis, avalanches, and acoustic emission associated to martensitic transitions in functional materials.'* arXiv:1009.2621

[4] M. Aizenman and J. Wehr, *'Rounding of First-Order Phase Transitions in Systems with Quenched Disorder'* Phys. Rev. Lett. **62**, 2503(1989)

[5] O. Perkovic, K. A. Dahmen, and J. P. Sethna, *'Disorder-Induced Critical Phenomena in Hystersis: A Numerical Scaling Analysis'*, cond-mat/9609072 *unpublished*

[6] D. Spasojević, Sanja Janićević, and Milan Knezević; *'Numerical Evidence for Critical Behavior of the Two-Dimensional Nonequilibrium Zero-Temperature Random Field Ising Model'*. Phys. Rev. Lett. **106**, 175701 (2011)

[7] D. Spasojević, Sanja Janićević, and Milan Knezević; *'Avalanche distributions in the two-dimensional nonequilibrium zero-temperature random field Ising model'* al Phys. Rev. E **84**, 051119 (2011)

[8] D. Spasojević, Sanja Janićević, and Milan Knezević; *'Analysis of spanning avalanches in the two-dimensional nonequilibrium zero-temperature random-field Ising model'*, Phys. Rev. E **89**, 012118 (2014)

[9] E.T Seppälä, V. Petäjä, and M. Alava, *'Disorder, Order, and Domain Wall Roughening in the 2d Random Field Ising Model'*, Phys. Rev. E **58**, R5217 (1998)

[10] B. Drossel and K. Dahmen, *'Depinning of a domain wall in the 2d random-field Ising model'*, Eur. Phys. J. B **3**, 485496 (1998)

[11] H. Ji and M.O. Robbins,*'Transition from compact to self-similar growth in disordered systems: Fluid invasion and magnetic-domain growth'* , Phys. Rev. A **44**, 2538 (1991)

[12] M.C. Kuntz, O.Perković, K.A. Dahmen, B.W. Roberts, and J.P. Sethna, *'Hysteresis, Avalanches, and Noise'* Comput. Sci. Eng. **July-August**, 73 (1999)

[13] E.D. Moore, R.B. Stinchcombe, and S.L.A. de Queiroz, *'Domain scaling and marginality breaking in the random-field Ising model'*, J. Phys. A **29**, 7409 (1996)

[14] S.V.Buldyrev, L.A.N. Amaral, A.L. Barabási, S.T Harrington, S. Halvin, J. Kertész, R. Sadr-Lahijany and H.E. Stanley; *'Avalanches in the directed percolation depinning and self-organized depinning models of interface roughening'* Fractals, **Vol. 4**, No. 3 (1996) 307-319

[15] H. Ji and M.O. Robbins, *'Percolative, self-affine, and faceted domain growth in random three-dimensional magnets'*, Phys. Rev. B **46**, 14519 (1992)